Langmuir
Article
pubs.acs.org/Langmuir

PM-IRRAS Assessment of the Compression-Mediated Orientation of the Nanocavity of a Monoacylated β-Cyclodextrin in Monolayers at the Air−Water Interface

Raquel V. Vico,*,† Rita H. de Rossi,‡ and Bruno Maggio†

†Centro de Investigaciones en Química Biológica de Córdoba (CIQUIBIC-UNC−CONICET), Departamento de Química Biológica and ‡Instituto de Investigaciones en Fisicoquímica de Córdoba (INFIQC-UNC−CONICET), Departamento de Química Orgánica, Facultad de Ciencias Químicas, Universidad Nacional de Córdoba, Haya de la Torre y Medina Allende, Ciudad Universitaria, X5000HUA, Córdoba, Argentina

Received December 23, 2009. Revised Manuscript Received February 22, 2010

The structural orientation adopted along the compression−decompression isotherm by a monoacylated β-cyclodextrin (C16-βCD) at the air−water interface was assessed by polarization-modulation infrared reflection-adsorption spectroscopy (PM-IRRAS). The adoption of different orientations of the cyclic oligosaccharide unit, relative to the interfacial plane, was interpreted analyzing the PM-IRRAS band intensity ratios of specific vibrations corresponding to the cyclodextrin moiety as a function of the surface pressure for successive compression/decompression cycles. The spectroscopic analysis revealed that the cyclic oligosaccharide modifies its position under compression from one in which the plane of the cavity of the monoacylated β-cyclodextrin lies almost parallel to the interface to another in which the plane of the cavity is perpendicular to the interface. Through the PM-IRRAS analysis, it was also possible to evidence the establishment of an intermolecular hydrogen bonding network that may play an important role in the dynamic properties of the monolayer packing. The hydrogen bonding network becomes more important with the increases of surface pressure, up to a molecular packing limit, and it imparts the surface properties of the film for future compression−decompression cycles.

Introduction

Cyclodextrins (CDs) are macrocyclic oligosaccharides capable of forming reversible non covalent complexes with a wide variety of guests, which allow them to function as all-purpose molecular containers.[1−5] The host−guest complex formation provides to the guest a different microenvironment that changes the physicochemical properties of the included molecule such as its chemical reactivity, stability, solubility, biodisponibility, and spectroscopic properties.[6−9] Because of that, important applications were found for their native forms as well as for some derivatives.[9−18]

Modified CDs were successfully applied in constructing molecular carriers and molecular platforms with important perspectives for nanoapplications.[5,9,12,19−23] For a successful design and application of CDs self-assemblies, a fundamental understanding of their self-structuring is crucial in order to provide a solid basis for their rational use in nanoconstruction. Different CDs derivatives have been prepared by substituting their primary or secondary hydroxyl groups thus obtaining highly amphiphilic compounds.[9,23−29]

*Corresponding author. Telephone: +54 351 4334168. Fax: +54 351 4334074. E-mail: rvico@mail.fcq.unc.edu.ar.

(1) Szejtli, J. *Chem. Rev.* **1998**, *98*, 1743–1754.
(2) Lim, C. W.; Ravoo, B. J.; Reinhoudt, D. N. *Chem. Commun.* **2005**, 5627–5629.
(3) Onclin, S.; Huskens, J.; Ravoo, B. J.; Reinhoudt, D. N. *Small* **2005**, *1*, 852–857.
(4) Voskuhl, J.; Ravoo, B. J. *Chem. Soc. Rev.* **2009**, *38*, 495–505.
(5) Frasconi, M.; Mazzei, F. *Nanotechnology* **2009**, 20285502.
(6) Vico, R. V.; Bujan, E. I.; de Rossi, R. H. *J. Phys. Org. Chem.* **2002**, *15*, 858–862.
(7) Vico, R. V.; de Rossi, R. H.; Buján, E. I. *J. Phys. Org. Chem.* **2009**, *22*, 691–702.
(8) Cruickshank, D.; Rougier, N. M.; Vico, R. V.; de Rossi, R. H.; Bujan, E. I.; Bourne, S. A.; Caira, M. R. *Carbohydr. Res.* **2010**, *345*, 141–147.
(9) *Cyclodextrins and their complexes. Chemistry, analytical methods, applications*; Dodziuk,H., Ed.; Wiley-VCH Verlag GmbH & Co.: Weinheim, Germany, 2006.
(10) Auletta, T.; Dordi, B.; Mulder, A.; Sartori, A.; Onclin, S.; Bruinink, C. M.; Peter, M.; Nijhuis, C. A.; Beijleveld, H.; Schonherr, H.; Vancso, G. J.; Casnati, A.; Ungaro, R.; Ravoo, B. J.; Huskens, J.; Reinhoudt, D. N. *Angew. Chem., Int. Ed. Engl.* **2004**, *43*, 369–373.
(11) Crespo-Biel, O.; Peter, M.; Bruinink, C. M.; Ravoo, B. J.; Reinhoudt, D. N.; Huskens, J. *Chem. Eur. J.* **2005**, *11*, 2426–2432.
(12) Dorokhin, D.; Hsu, S. H.; Tomczak, N.; Reinhoudt, D. N.; Huskens, J.; Velders, A. H.; Vancso, G. J. *ACS Nano* **2010**, *4*, 137–142.
(13) Du, L.; Liao, S.; Khatib, H. A.; Stoddart, J. F.; Zink, J. I. *J. Am. Chem. Soc.* **2009**, *131*, 15136–15142.
(14) Falvey, P.; Lim, C. W.; Darcy, R.; Revermann, T.; Karst, U.; Giesbers, M.; Marcelis, A. T.; Lazar, A.; Coleman, A. W.; Reinhoudt, D. N.; Ravoo, B. J. *Chemistry* **2005**, *11*, 1171–1180.
(15) Hernandez-Pascacio, J.; Garza, C.; Banquy, X.; Diaz-Vergara, N.; Amigo, A.; Ramos, S.; Castillo, R.; Costas, M.; Piñeiro, A. *J. Phys. Chem. B* **2007**, *111*, 12625–12630.
(16) Ludden, M. J.; Li, X.; Greve, J.; van, A. A.; Escalante, M.; Subramaniam, V.; Reinhoudt, D. N.; Huskens, J. *J. Am. Chem. Soc.* **2008**, *130*, 6964–6973.
(17) Perl, A.; Kumprecht, L.; Kraus, T.; Armspach, D.; Matt, D.; Reinhoudt, D. N.; Huskens, J. *Langmuir* **2009**, *25*, 1534–1539.
(18) Versluis, F.; Tomatsu, I.; Kehr, S.; Fregonese, C.; Tepper, A. W.; Stuart, M. C.; Ravoo, B. J.; Koning, R. I.; Kros, A. *J. Am. Chem. Soc.* **2009**, *131*, 13186–13187.
(19) Freeman, R.; Finder, T.; Bahshi, L.; Willner, I. *Nano. Lett.* **2009**, *9*, 2073–2076.
(20) Maury, P.; Péter, M.; Crespo-Biel, O.; Ling, X. Y.; Reinhoudt, D. N.; Huskens, J. *Nanotechnology* **2007**, *18*, 044007.
(21) Patel, K.; Angelos, S.; Dichtel, W. R.; Coskun, A.; Yang, Y. W.; Zink, J. I.; Stoddart, J. F. *J. Am. Chem. Soc.* **2008**, *130*, 2382–2383.
(22) Ferris, D. P.; Zhao, Y. L.; Khashab, N. M.; Khatib, H. A.; Stoddart, J. F.; Zink, J. I. *J. Am. Chem. Soc.* **2009**, *131*, 1686–1688.
(23) Cristiano, A.; Lim, C. W.; Rozkiewicz, D. I.; Reinhoudt, D. N.; Ravoo, B. J. *Langmuir* **2007**, *23*, 8944–8949.
(24) de Rossi, R. H.; Silva, O. F.; Vico, R. V.; Gonzalez, C. J. *Pure Appl. Chem.* **2009**, *81*, 755–765.
(25) Roux, M.; Perly, B.; Djedaïni-Pilard, F. *Eur. Biophys. J.* **2007**, *36*, 861–867.
(26) Silva, O. F.; Fernandez, M. A.; Pennie, S. L.; Gil, R. R.; de Rossi, R. H. *Langmuir* **2008**, *24*, 3718–3726.
(27) Vico, R. V.; Silva, O. F.; de Rossi, R. H.; Maggio, B. *Langmuir* **2008**, *24*, 7867–7874.
(28) Tchoreloff, P. C.; Boissonnade, M. M.; Coleman, A. W.; Baszkin, A. *Langmuir* **1995**, *11*, 191–196.
(29) Zhang, P.; Parrot-Lopez, H.; Tchoreloff, P. C.; Baszkin, A.; Ling, C.-C.; De Rango, C.; Coleman, A. W. *J. Phys. Org. Chem.* **1992**, *5*, 518–528.

Scheme 1. (A) Chemical Structure of Mono-Acylated β-Cyclodextrin C16-βCD and (B) the Orientation of the Oligosaccharide Ring[a]

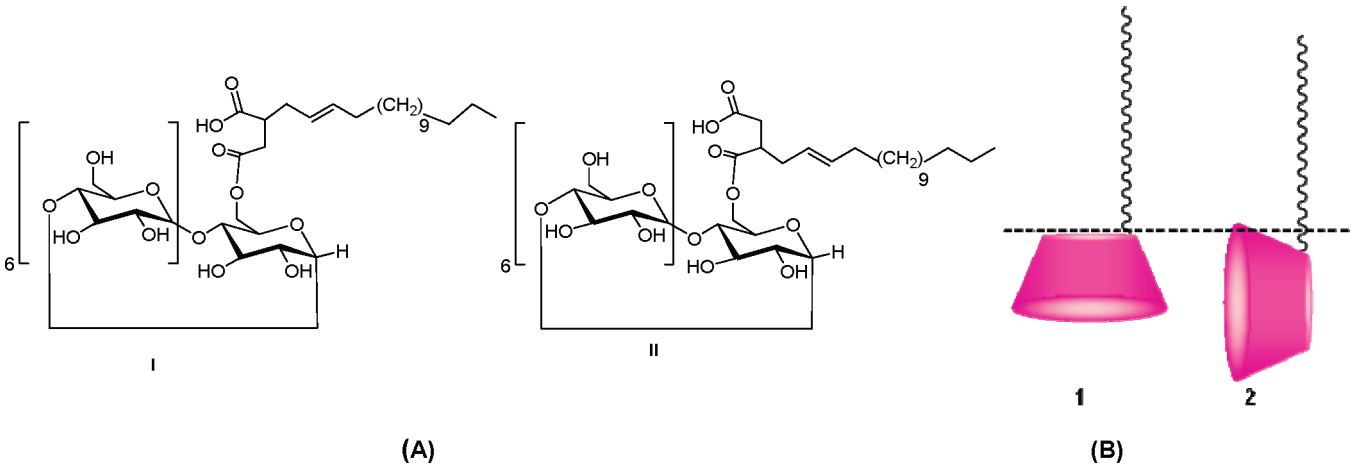

[a] In part A, I and II represent the two isomers obtained during the syntheses of C16-βCD where the alkenyl chain is in position 3 (for I) and in position 2 (for II) respect to the carboxyl group linked to the β-cyclodextrin. In part B, the orientation of the oligosaccharide ring of C16-βCD is represented as a cartoon, with the plane of the cavity oriented parallel (1) and perpendicular (2) to the interface. The horizontal dashed line corresponds to the approximate position of the air-aqueous interface.

The full substitution of cyclodextrins leads to rigid cylindrical structures that are very anisotropic regarding the vectorial separation of the hydrophobic and hydrophilic moieties. This confers to these molecules a rather high stability when organized in monolayers at the air-aqueous interface. However, full substitution also confers scarce conformational flexibility and therefore little possibilities for adopting different intermolecular arrangements in the monomolecular film.[25,28,29]

We recently reported that the presence of a single hydrocarbon chain linked to one glucopyranose unit in the cyclodextrin ring brings about more possibilities for different organizations depending on the lateral surface pressure.[27] The films formed by the amphiphilic cyclodextrin C16-βCD (Scheme 1) show distinctive structural features such as variations of the surface packing, dipole moment reorientation and surface topography; this suggested the likely occurrence of reorientation of the βCD rim to the aqueous milieu leading to different interfacial organizations at different lateral surface pressures. Also, it was found that the organization adopted by the film at a defined surface pressure depended on whether or not the film was previously compressed; this was clearly revealed by the presence of packing hysteresis with the consequent potential for structural information storage.[27] The specific orientation acquired by the oligosaccharide rim of C16-βCD as a function of surface pressure was more precisely inspected by using the variation of the PM-IRRAS band intensity ratios corresponding to specific vibrations of the cyclodextrin moiety.

The selection rules of PM-IRRAS spectroscopy at the air−water interface allow determining the orientation of the transition moments of vibrational modes relative to the interface. The up (down) sense of a band relative to the baseline and its intensity are dependent on the orientation of the corresponding transition. If the transition moment is parallel to the interface the absorption results in a strong positive band, whereas the band is negative if the transition moment is perpendicular to the surface. Between these two extreme cases an intermediate orientation of the transition moment will led to compensated positive and negative contributions thus affecting specific band relationships.[30,31]

For β-cyclodextrin (βCD), the direction of these transition moments relative to the axes of the macrocycle have recently been determined.[32] The most important region in the IR spectra is located in the 1300−900 cm^{-1} range. For βCD there are two intense bands located at 1030 (1026 in our system) and 1172 (1165 in our system) cm^{-1}. According to the above study, the mode at 1030 cm^{-1} is essentially located in the $x-y$ plane of the βCD molecule, whereas the other one at 1172 cm^{-1} contains an important contribution along the z axis.[32]

As far as we know, no structural data concerning the specific structural orientation and intermolecular interaction of the cyclic oligosaccharide of amphiphilic cyclodextrin films have been reported to date. In this report we provide an insight on some details of the structural reorganizations that occur in monolayers of a monoacylated β-CD throughout the isothermal compression−decompression cycles. The current PM-IRRAS results further support previously described studies of their surface reorganization under film compression−decompression.[27]

Materials and Methods

The monoacylated cyclodextrin C16-βCD (Scheme 1A) was synthesized and purified following methodology reported elsewhere.[26,27] The degree of substitution was determined by ^{1}H NMR spectroscopy by relating the ^{1}H NMR signals corresponding to the protons of the methyl group in the alkenylic chain and the anomeric protons of glucoses of β-cyclodextrin, respectively.[26,27] The degree of substitution determined for C16-βCD was 1.5; this means that the preparation, contained an *average* of 50% of molecules with one and 50% of molecules with two acyl chains for C16-βCD.[27] ^{1}H NMR and ^{13}C NMR experiments were run using high-resolution spectrometer Bruker Advances II 400, or Bruker AC 200 instruments.

The organic solvents were of the highest purity available (Merck). Water was of Milli-Q quality (Millipore System). NaCl was roasted at 400 °C for 4 h. To form the films, monoacylated cyclodextrin was spread from a chloroform−methanol−dimethyl sulfoxide (1:1:1) solution. Langmuir monolayers were formed by spreading the stock solution of the monoacylated cyclodextrin, and 5 min were allowed before starting compression. Monolayers were obtained at room temperature (23−25 °C) by spreading less

(30) Buffeteau, T.; Blaudez, D.; Péré, E.; Desbat, B. *J. Phys. Chem. B* **1999**, *103*, 5020–5027.
(31) Blaudez, D.; Turlet, J.-M.; Dufourcq, J.; Bard, D.; Buffeteau, T.; Desbat, B. *J. Chem. Soc. Faraday Trans.* **1996**, *92*, 525–530.
(32) Mascetti, J.; Castano, S.; Cavagnat, D.; Desbat, B. *Langmuir* **2008**, *24*, 9616–9622.

than 15 μL of a stock solution on the surface (273 cm^2) of a 145 mM NaCl subphase of a KSV minithrough equipment (KSV, Helsinki, Finland) at a compression rate of 10 mm/min. Absence of surface active impurities in the spreading solvent and aqueous subphase was routinely checked before each run as discussed elsewhere.[27]

Polarization−modulation infrared reflection absorption spectroscopy (PM-IRRAS) was performed using a KSV PMI 550 instrument (KSV Instruments Ltd., Helsinki, Filand) which contains a compact Fourier Transform IR-spectrometer. One arm of the goniometer bears a PM-unit (ZnSe photoelastic modulator) and a highly sensitive MCT detector is mounted on the other arm. The spectra were acquired with a resolution of 8 cm^{-1} over a spectral range of 800−4000 cm^{-1}. The Langmuir trough was set up so that the light beam reached the monolayer at a fixed angle of incidence of 80°and the frequency of wavelength modulation used was 1500 cm^{-1}. The incident light was continuously modulated between s and p polarization at a high frequency ($2f$ = 100 kHz). This allows the simultaneous measurement providing the reference spectrum. Because the spectra are measured simultaneously the effect of water is largely reduced. The baseline was acquired using a film-free NaCl 145 mM solution. Each spectrum was obtained with 6000 scans accumulation at a temperature of 23−25 °C.

The PM-IRRAS spectra were normalized by using the Origin 7.0 software. The normalization procedure was performed by rescaling the spectral region at 890−1700 cm^{-1} (βCD region) and at 2700−3000 cm^{-1} (hydrocarbon chain region): values of 0 and 1 were assigned to the lowest and highest band intensities, respectively, at each surface pressure. The PM-IRRAS spectra shown were obtained from the average of at least three normalized spectra, each resulting from the accumulated 6000 scans. For decompression experiments, the films were compressed up to a surface pressure of 40 mN/m and decompressed to the desired surface pressure at a compression−decompression rate of 10 mm/min.

Absorbance FTIR spectra of βCD and C16-βCD powder (mixed with KBr) were measured in a Nicolet 5XC spectrophotometer.

Brewster Angle Microscopy (BAM) images of the C16-βCD film were obtained with an EP^3−BAM (Nanofilm Technologie GmbH, Göttingen, Germany) using a 20× objective. Images were captured with a cooled charge-coupled device (CCD) camera with a speed of 25 Hz. The wavelength of the laser beam was 532 nm and the angle of incidence was set at 53.1°. The surface pressure was measured with a small Langmuir trough (Nima Technology, Coventry, U.K.) mounted under the microscope.

Results and Discussion

PM-IRRAS spectroscopy was employed in order to obtain specific molecular information regarding the possible orientation of the βCD moiety resulting from the intermolecular organization adopted in the C16-βCD film under compression.

As described for βCD there are two intense bands, one at 1030 (1026 in our system) cm^{-1} essentially located in the $x-y$ plane and the other at 1172 (1165 in our system) cm^{-1} that has an important contribution along the z axis.[32] According to this, among other things, an oriented channel-like structure of stacked βCD rings (each moiety with the plane of the cavity parallel to the surface) located perpendicular to the air−water interface was conceived as the structure involved in extracting cholesterol from a cholesterol monolayer.[32] For such orientation of the βCD ring almost parallel to the interface the PM-IRRAS spectrum exhibits an intense low-wavenumber mode; in this orientation, the transition moment of the 1172 cm^{-1} mode is more perpendicular to the surface and the intensity is diminished compared to that of the 1030 cm^{-1} mode which has a greater x-y component parallel to the surface.[32]

The IR powder spectra of βCD and C16-βCD (Figure 1) show intense and sharp bands in the range 1170−890 cm^{-1}, which can be associated with the primary and secondary C−OH groups stretching frcuency of the cyclodextrin.[33] Additionally, the C16-βCD IR spectrum shows the band corresponding to the C═O groups at 1728 cm^{-1} (see Scheme 1A).

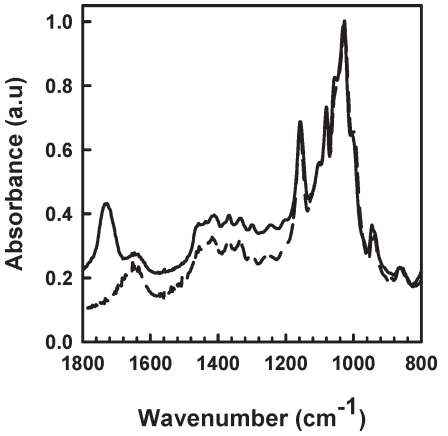

Figure 1. Normalized absorbance IR spectra of βCD (dashed line) and C16-βCD (solid line) powder.

Figure 2 shows the PM-IRRAS spectra of C16-βCD monolayer at different surface pressures during the first compression isotherm. The PM-IRRAS spectra of C16-βCD film at different surface pressures show that at low surface pressures (up to 10 mN/M) the 1026 cm^{-1} mode is stronger than that at 1165 cm^{-1}, consistent with the βCD ring laying almost parallel to the surface, see Scheme 1B. As the film is compressed above that pressure, the intensity of the band at 1165 cm^{-1} increases more than that of the signal located at 1026 cm^{-1}; this fact is clearly revealed by taking the ratio of the two band intensities (Figure 3A). From the ratio of the bands (1026/1165) it can be seen that up to 10 mN/m the relationship remains almost constant and for higher surface pressures it diminishes to a minimum at a surface pressure of about 36 mN/m and then it increases again (see below). The trend in the relationship of these two modes clearly indicates that the βCD ring rearranges its position from one with the plane of the cavity mostly parallel, to another tending to be approximately perpendicular to the interface between 10 and 36 mN/m (see Scheme 1B). This behavior is in agreement with the changes shown by other surface parameters previously studied to characterize the surface behavior of the film formed by C16-βCD.[27]

Another distinctive feature that is observed in the PM-IRRAS spectra of the C16-βCD film (Figure 2A) is the appearance of a band at 1265 cm^{-1} which rapidly increases its magnitude with the increment of surface pressure. In Figure 1 it can be seen that such band is not found in the solid powder spectrum of C16-βCD. From the monolayer behavior in terms of molecular packing, dipole potential and in-plane elasticity we previously concluded that, as the surface pressure is increased, the C16-βCD molecules in the film interact among them and remain closely packed in clusters after the first compression.[27] The clustering of the C16-βCD molecules could result from the capability of the cyclodextrins to form intermolecular hydrogen bonds;[24,27] hydrogen bond short-range interactions between stacked βCD rings have been reported.[15] The PM-IRRAS experiments reveal that, once the C16-βCD molecules are close enough to interact and the ring had adopted the proper orientation in the film, an intermolecular hydrogen bonding network is established. The band observed at

(33) Villaverde, J.; Morillo, E.; Pérez-Martínez, J. I.; Ginés, J. M.; Maqueda, C. *J. Agric. Food Chem.* **2004**, *52*, 864–869.

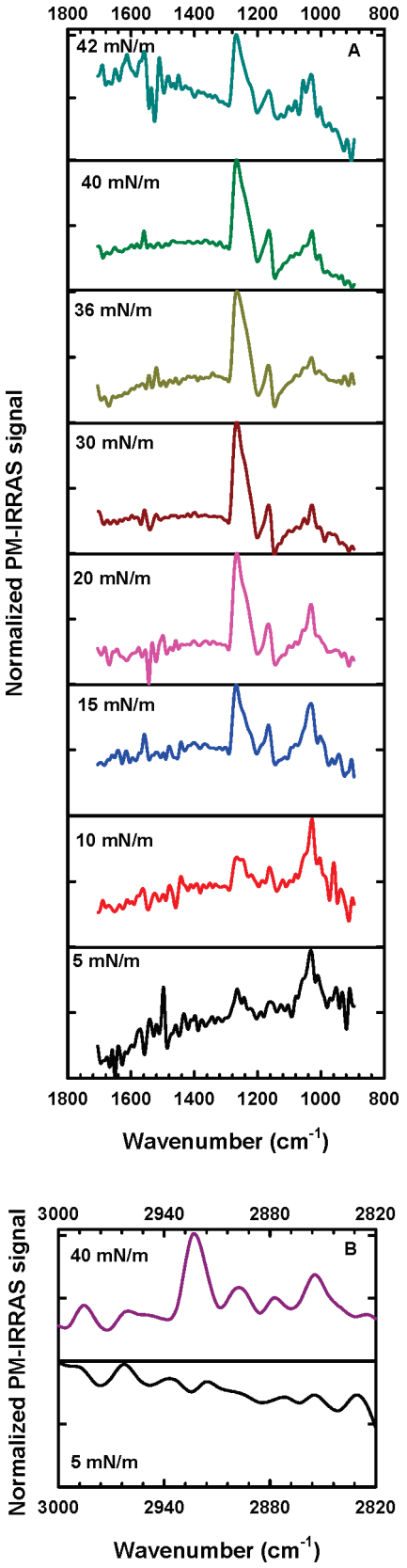

Figure 2. Normalized PM-IRRAS spectra of C16-βCD film at different surface pressure during the first compression. (A) βCD ring region and (B) hydrocarbon chain region showing the symmetric (ν_s CH_2) and antisymmetric (ν_a CH_2) stretching bands of the methylene groups. The normalized scale for each spectrum is from 0 to 1, and each tick mark in the graphs corresponds to 0.5 normalized units (see Materials and Methods) representing approximately 0.015 PM-IRRAS signal units.

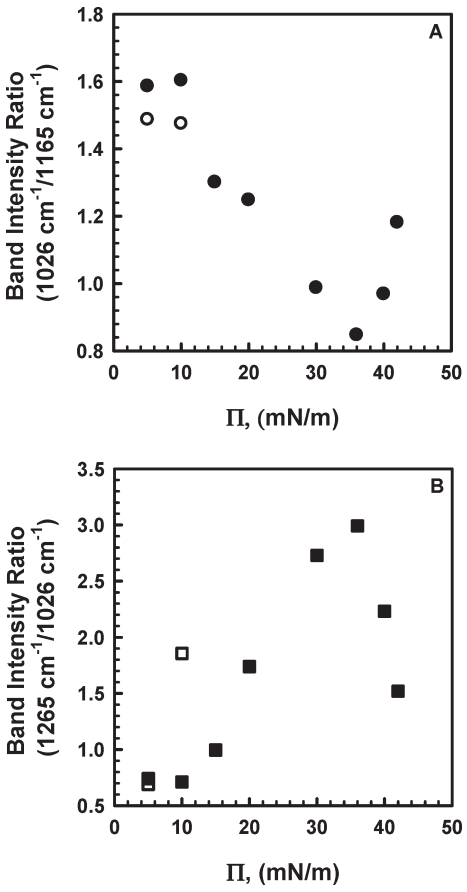

Figure 3. PM-IRRAS band intensity ratio for the modes at 1026/1165 cm^{-1} (A) and 1265/1026 cm^{-1} (B) obtained during the first compression (filled symbols) and first decompression (unfilled symbols) isotherms of the C16-βCD monolayer.

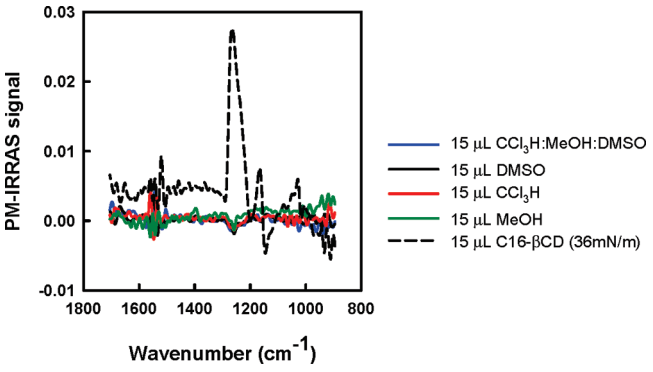

Figure 4. PM-IRRAS spectra of C16-βCD compressed up to 36 mN/m (dashed line) and of the 1:1:1 (CCl_3H:MeOH:DMSO) mixture and each of this solvents separately (solid lines) spread over a NaCl 145 mM subphase.

1265 cm^{-1} likely result from the establishment of such intermolecular hydrogen bonding network. Figure 3B shows the intensity relationship between the 1265 and 1026 cm^{-1} bands. The band intensity ratio remains nearly constant up to 10 mN/m, it increases above this surface pressure and reaches the highest value at 36 mN/m, diminishing again at higher surface pressures (see below). Proper controls were done by spreading on the surface the solvent mixture (CCl_3H:MeOH:DMSO, 1:1:1) or each of these solvents separately. For each individual solvent or for the solvent mixture only a very small signal at 1265 cm^{-1} was observed (with

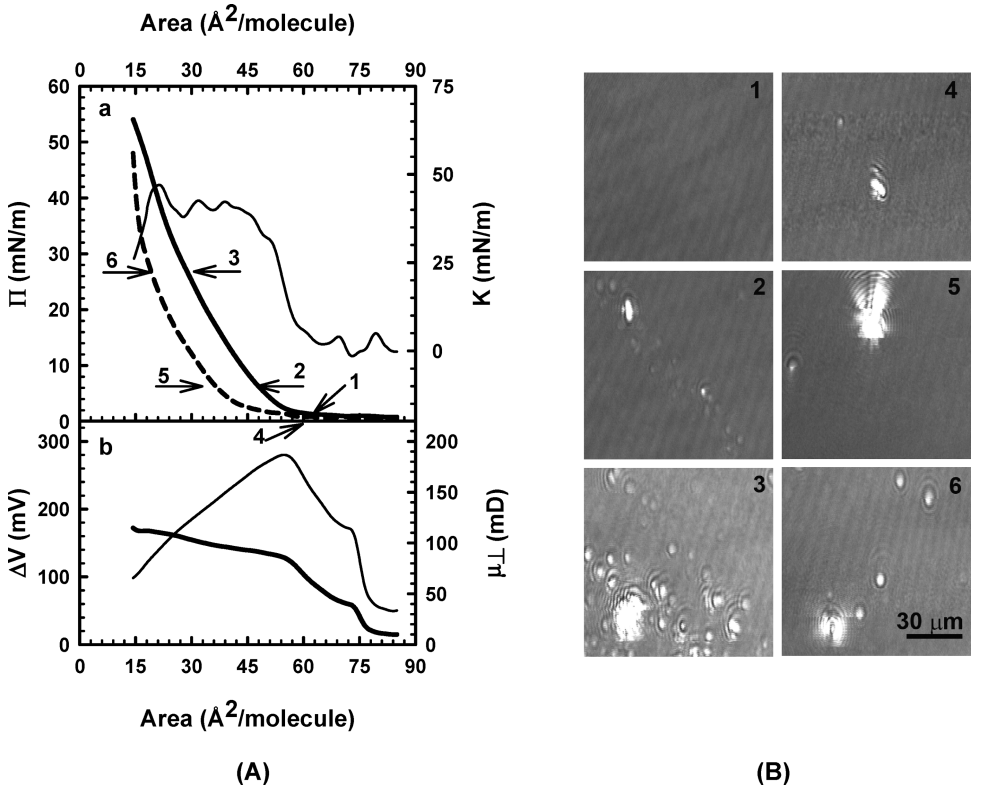

Figure 5. (A) (a) Variation of surface pressure (thick lines) and surface compressional modulus, K, (thin lines) with molecular area for C16-βCD, first compression (solid line), first decompression (dashed line). (b) Variation of surface potential (thick lines) and perpendicular resultant dipole moment, $\mu_{\perp}$, (thin line) with molecular area for the first compression. (B) BAM images showing the lateral topography of the C16-βCD film spread on 145 mM NaCl subphase. Micrographs were obtained at 1 mN/m, 7 and 27 mN/m during the first compression (1, 2, 3) and the first decompression (4, 5, 6), respectively; numbers on the photographs in panel B correspond to those indicated on the isotherms in panel A. The film was compressed up to a surface pressure of 39 mN/m and decompressed. The film-free subphase did not show any reflectance inhomogeneities.

respect to the background noise) but oriented negatively with respect to the baseline. Thus, the band at 1265 cm^{-1} is not due to the spreading solvent since this is completely different to the positive band given by the film of C16-βCD (Figure 4).

Also, as the surface pressure raises, the methylene and methyl bands from the hydrocarbon chain increase in intensity as expected for the increment in the molecular surface density (Figure 2B).

It was previously shown that, once the monolayer has been compressed to the closest packing, the film shows variations in the intermolecular packing, surface potential, in-plane elasticity, and surface reflectance and topography;[27] the first decompression shows a much more condensed film and the molecules remain closely packed in a liquid condensed state and clustered arrays of high reflectance remain even at very low surface pressures, compared to the first compression (Figure 5). The PM-IRRAS spectra also reveal the close and clustered packing maintained along the decompression isotherm. At a surface pressure of 10 mN/m (and also at 5 mN/m) the band at 1265 cm^{-1}, due to the intermolecular hydrogen bonding network, remains more intense in the decompression isotherm than during the first compression as evidenced by the relationship of the (1265/1026) cm^{-1} modes (Figure 3B and Figure 6).

It is important to point out that the marked changes of the PM-IRRAS band intensity ratios with the surface pressure occur at mean molecular areas that are in coincidence with the changes of intermolecular organization revealed by the surface pressure and surface potential isotherm, the surface compressional modulus, and the reflectance previously reported.[27]

During the first compression, at about 5 mN/m and molecular packing less than 50 $Å^2$ the film enters into a liquid condensed state. As the molecules become more closely packed, the film remains in a similar liquid condensed state, from a surface pressure of 5 mN/m to about 30 mN/m (about 50 to 28 $Å^2$, see Figure 5Aa). This is revealed by the approximate plateau values of the surface compressional modulus K (with values between 30 and 40 mN/m) which correspond to in-plane elasticities of films having a rather condensed solid state.[27] At about 35 mN/m (24−23 $Å^2$) a new change of slope of the resultant perpendicular dipole moment vector-molecular area isotherm (Figure 5Ab) occurs in a very condensed film; the enhancement of the solid-like state is clearly noticeable by the further increase of the in-plane elasticity (reproducible peak of the surface compressional modulus of about 48 mN/m, see Figure 5Aa) occurring at about 24 $Å^2$ and 35 mN/m. All these changes are in coincidence with the changes in trend of the band intensity ratios shown in Figure 3.

The inversion of the tendencies of the band intensity ratio with the increase of surface pressure above 36 mN/m shown in Figure 3 deserves some additional comments. For this, it is necessary to take into account data previously reported regarding the mean molecular area, the variation of the molecular dipole moment perpendicular to the interface, and the further variation of the in-plane elasticity (compressibility modulus) detected at the surface pressure at which the band intensity ratios are inverted (see Figure 3 and 5).[27]

It is clear that beyond about 36 mN/m (22 $Å^2$) the βCD ring, even with the plane of the cavity oriented, on average, perpendicular to the interface, can no longer fit under the cross-sectional

area covered by the closely packed hydrocarbon chain[27] (see Scheme 1B and 2A). In such over compressed state relative molecular displacements or tiltings have to take place (the equilibrium adsorption pressure of C16-βCD is 38 ± 1 mN/m[27]). Such reorganizations and/or molecular dislocations with respect to the interfacial plane attained at very high surface pressures are reflected by other two independent parameters measured in the film: a further increase of the surface rigidity shown by the in-plane elasticity and a further change of slope of the resultant perpendicular dipole moment occurring at molecular packings smaller than about 30 Å^2. In agreement with these observations (see Figure 5), the optical evidence previously reported reveals the formation of rigid clusters of high reflectivity at such high surface pressures that also suggest the occurrence of perpendicular dislocations out of the interfacial plane.[27]

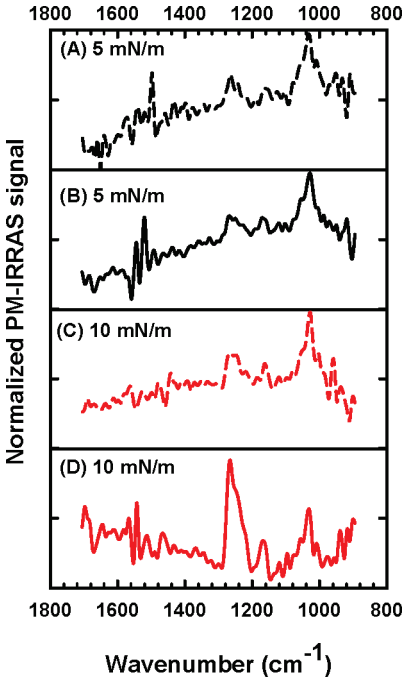

Figure 6. Normalized PM-IRRAS spectra of the C16-βCD film obtained during the first compression (dashed line) and first decompression (solid line) at 5 mN/m (A y B) and 10 mN/m (C y D). The normalized scale for each spectrum is from 0 to 1, and each tick mark in the graphs corresponds to 0.5 normalized units (see Materials and Methods) representing approximately 0.015 PM-IRRAS signal units.

In keeping with all the above, the further increase of the band intensity ratio 1026/1165 beyond 36 mN/m, may indicate a vertical displacement of the βCD ring (oriented mostly perpendicular to the interface) with partial lateral stacking of the oligosaccharide moiety (see Scheme 2B). Concurrently, the decrease of the band intensity ratio 1265/1026 indicates that the side-to-side hydrogen bonding network formed among laterally stacked βCD rings is diminished, which would be consistent with their vertical dislocation out of the interfacial plane (see Scheme 2B). The maximal value of the 1265/1026 intensity ratio occurs at about the equilibrium adsorption pressure (38 mN/m) of C16-βCD, indicating that the molecules self-organize at the interface maximizing the hydrogen bonding network.

Conclusions

By PM-IRRAS analysis, it was possible to obtain detailed structural data referred to the reorientation and intermolecular interaction of amphiphilic cyclodextrin in a self-organized monolayer at the air−water interface under compression. Furthermore, with this spectroscopic technique it was possible to disclose the establishment of an intermolecular hydrogen bonding network and surface dislocation among βCDs rings that may be important for explaining the dynamic behavior of the film regarding its intermolecular packing and the hysteresis observed under successive compression/expansion cycles. It emerged from this study that the hydrogen bonding network becomes more important as the surface pressure is increased, suggesting that it can be an important factor controlling the reversibility of the surface properties of the film.[27]

The properties displayed by the C16-βCD monolayer film are of considerable interest in nanoscience and nanotechnology focused on the development of functional materials and self-organized surfaces for applications as nanoreactors, (bio)sensors, electronical and optical devices as well as surface sequestration of ligands. The distinctive feature shown by the C16-βCD film, such as the capability of storing chemical intermolecular information and programmability under defined molecular organization on the nanoscale attained under

Scheme 2. (A) CPK Space Filling Model of C16-βCD in the Closely Packed State and (B) Illustration of Molecular Orientation Adopted by C16-βCD along the Compression/Decompression Isotherm[a]

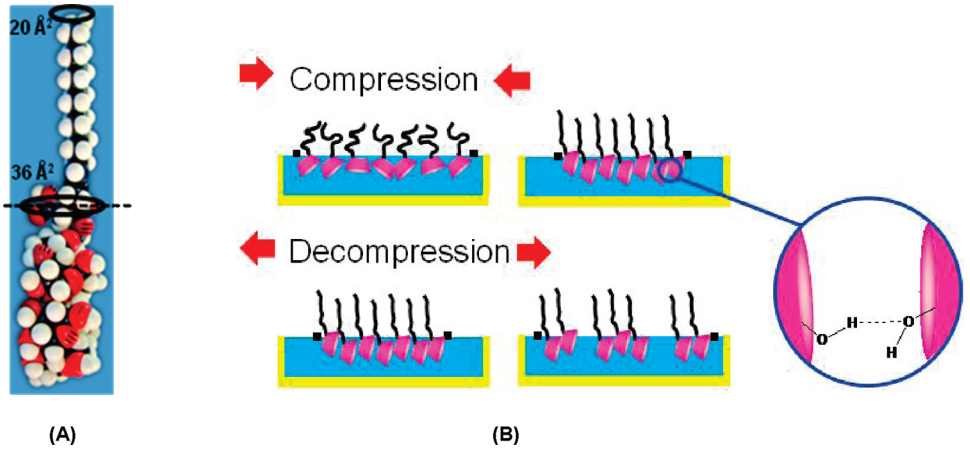

[a] The schematic representation shows the likely reorganizations and/or molecular dislocations and clustering that may take place. The inset shows possible hydrogen bonding among adjacent molecules.

compression/decompression, could be used to structurally control noncovalent interactions of the CD nanocavity with specific guests, depending on the cavity constraints and exposure imposed by the lateral packing.

Acknowledgment. This work was supported by SECyT-UNC, CONICET, FONCYT, and MINCyT Argentina. R.V.V. is a postdoctoral fellow of CONICET. B.M. and R.H.deR. are Career Investigators of CONICET.